AN INVESTIGATION ON NANO-STRUCTURED SANDWICH PANELS DAMAGE TOLERANCE

Antonio F. Ávila, aavila@netuno.lcc.ufmg.br
Maria Gabriela R. Carvalho, mariagabrielacarvalho@yahoo.com.br
Eder C. Dias, edercesar01@gmail.com
Diego T.L. da Cruz, dtlcruz@gmail.com
Universidade Federal de Minas Gerais, Department of Mechanical Engineering and Graduate Program on Mechanical Engineering (PPGMEC-UFMG), 6627 Antonio Carlos Avenue , Belo Horizonte, MG 31270-901, Brazil

Abstract. *The aim of this paper is to investigate the influence of nano-structures, mostly intercalated form, on sandwich composites under impact loadings. To achieve such goal, a set of sandwich composites plates made of fiberglass/nano-modified epoxy face sheets and polystyrene foams was prepared. The polystyrene core was 25 mm thick and the face sheets were made of eight layers of woven fabric glass fibers and nano-modified epoxy (≈ 0.8 mm of thickness). The epoxy system was made of bisphenol A resin and an amine hardener, i.e. RemLam M and HY956, from Hunstman Inc. The fiber volume fraction used was around 65%, while the nanoclay content varied from 0 wt% to 10 wt%. The nanoclay used in this research was organic modified montmorillonite produced by Southern Clay Inc. (Cloisite 30B). Once the sandwich composites planes were prepared, they were submitted to low velocity impact tests using a drop weight tower. The energies applied ranged from 5 Joules to 75 Joules. Two sets of experiments were performed, i.e. high velocity + low mass and low velocity + high mass. Damage caused by the two groups of experiments and peak forces measured were dissimilar. The results show that the addition of 5% on nanoclay with respect to the epoxy system weight leads to a more efficient energy absorption and a different failure modes. Two transition failure modes, from upper face sheet cracking + core indentation to upper face sheet tearing + core crushing, and upper face sheet tearing + core crushing to lower face sheet and core debonding, appears to overshadow the nanoclay effect, as they seems to be infective in these two conditions.*

Keywords*: nanostructured materials, sandwich structures, nanoclay, impact loading, damage tolerance.*

1. INTRODUCTION

As mentioned by Schubel et al. (2005), the use of composite sandwich structures is increasing in the aerospace and marine industry, as well as in other areas where a lightweight material with elevated flexural stiffness is required. The design concept behind these structures is the increase in flexural stiffness by placing two stiff, strong and thin face sheets estranged by a lightweight thicker flexible core. By employing this strategy, the moment of inertia is enhanced and consequently the flexural properties increase while keeping the weight practically unaffected. According to Vinson (1999), as face sheets carry most of the load, an optimal design for sandwich composite structures must take into consideration the face sheet response to static and dynamic loads. Unfortunately, as discussed by Lim and his coworkers (2004), most of the previous studies have focused on the strength capacity of sandwich structures under quasi-static loading. However, Abrate (2001) called attention to the response of sandwich composite structures to impact loadings. According to him, this class of structures is susceptible damage caused by foreign objects impact. The composite sandwich structures response to low velocity impact have been the focus of various researchers.

As described by Mines and his colleagues (1998), the low velocity impact of composite sandwich panels (to this investigation structures and panels have the same meaning) covers the response from sub-critical damage to full perforation. Furthermore, an important point of interest investigated by Mines et al. (1998) was the relationship between the peak impact force and the damaged area. They concluded that core density has direct influence on damage propagation and energy absorption. Another issue, i.e. the sandwich composite rate-sensitivity, was investigated by Hazizan and Cantwell (2002). They demonstrated that foam based sandwich composites are insensitive to crosshead displacement rate over a large range (0.1 – 1000 mm/min). Ávila (2007) has shown that by varying the sandwich composite core density, as in functionally graded sandwich structures, damage mechanism also changes as function of density distribution. Laurin and Vizzini (2005) went further, as they demonstrated that by placing graphite/epoxy reinforcement through-thickness in a foam core enhances the normal energy absorption of foam-core sandwich structures. Still, they called our attention to the fact that there is no linear relationship between the increase on energy absorption and the addition of stiffness introduced. Suvorov and Dvorak (2005) also tried to enhance the sandwich energy absorption by placing an interlayer material between the face sheet and the foam core. Their mathematical model seems to be encouraging. Nevertheless, no experimental data was provided to validate the model.

Ávila et al. (2006) showed that failure mechanisms of laminated composites (in the present investigation face sheets) can be influenced by nano-structures formed by nanoparticles dispersed into epoxy systems. According to them, the presence of nanoclay into fiber glass/epoxy composites lead to a more intense formation of delaminated areas after a low velocity impact test (LVI). This phenomenon was attributed to interlaminar shear forces caused by the intercalated nano-structures inside the epoxy system. Furthermore, the energy absorption of these laminates increased by 48% with

dispersion of 5 wt% of nanoclays. Another important issue described by Li et al. (2006) is that, when sandwich composites were submitted to LVI tests, there was impact weave propagation inside the two distinct materials, i.e. face sheets and core. Ávila et al. (2007) demonstrated that nano-modified laminated composites had their natural frequencies altered by nano-structures formed inside the laminated. A crossing mode, 4th mode higher than the 3rd mode, was reported by Ávila et al. (2007) with the addition of 5 wt% of montmorillonite to fiber glass/epoxy laminates.

This paper focus on the effect of nanoclay dispersed into an epoxy/fiber glass composite and its influence on the sandwich composites response to low velocity impact tests.

2. EXPERIMENTAL PROCEDURES

2.1 Constitutive materials and fabrication

Ten sandwich panels were evaluated during the course of this research. The face sheets of the sandwich panel were fiber glass/nano-modified epoxy system laminates. The epoxy system was made of *bisphenol A* resin and an amine hardener, i.e. RemLam M and HY956, from Hunstman Inc. The nanoclay used in this research was organic modified montmorillonite produced by Nanocor Inc. (Nanomer I30E). The nanoclay content employed was 0 wt% (control), 1 wt%, 2 wt%, 5 wt% and 10 wt%. Eight layers of plain weave woven fabric fiber glass with aerial density of 200 g/m^2 were employed, resulting in a cured plate with thickness of 0.8 mm and a fiber volume ratio of 0.65. The core used for the sandwich panel was closed-cell PS foam (Styrofoam obtained from Dow). This foam has a density of 35 kg/m^3. The core was 25.4 mm thick.

During the face sheet preparation, the nanoclay dispersion process into the epoxy system followed the procedure describe in Ávila et al. (2008). A dispersant agent, acetone, was employed to improve the mixing process. The degassing stage was required to eliminate bubbles generated during the mechanical mixing, as well as to eliminate the dispersant agent, i.e. acetone. After this procedure, the hand lay-up with vacuum assisted cure was performed.
The sandwich panel was fabricated by bonding the cured face sheets to the core material with the same epoxy system applied during the laminate consolidation. A vacuum bagging technique was used to ensure a uniform pressure during the bonding procedure. The final sandwich panel was a square plate of 30 x 30 cm dimensions with an overall thickness of 2.70 cm and mass of 0.52 kg.

2.2 Nanoclay detection tests

According to Koo (2006), during the nanoparticles dispersion into polymeric matrices nano-structures are formed. The two most common detection techniques to nano-structures identification are X-ray diffraction and electronic microscopy. In this research, X-ray diffraction (XRD) experiments were carried out on a Shimadzu XRD-6000 X-ray diffract meter with Cu (λ=0.154 nm) irradiation at 40 *kV* and 30 *mA* using a Ni filter. Data were recorded in the range from 2 to 80 deg in a continuous scanning at 2 degrees per minute and sampling pitch of 0.02 deg. The scanning electron microscope (SEM) used was a LEO model 1430VP. In all cases, a gold thin film was placed on the surface of the sample to able to scan its structure. Finally, a thermal stability analysis was also performed using a Shimadzu DTG 60 Thermogravimeter under nitrogen, at 10 C/min from 25 C to 750 C. As this research deals with dynamic loadings, in addition to the traditional nanoparticles dispersion analysis, information about the sandwich response under indentation must be supplied.

2.3 Indentation testing

According to Hazizan and Cantwell (2002), during impact events sandwich structures absorb significant energy in contact deformations around the impact area. Thus, a series of indentation tests were carried out using an INSTRON universal testing machine at crosshead displacement rate of 0.2 mm/min. The indentation tests were conducted using a hemi-spherical indentor of 10 mm diameter. The sandwich panels were loaded up to a force with same magnitude of the ones recorded during the low velocity impact tests. As described by Abrate (2001), during the loading phase of the impact, the contact force P is related to the indentation α by

$$P = C\alpha^n \tag{1}$$

The load-indentation data were fitted to this equation to yield the values of n and C for each group of sandwich panels.

3. IMPACT LOADING MODELING

Once the sandwich panels were manufactured and the indentation tests were carried out, the impact resistance test by falling dart can be performed. Following the ASTM D 5628-01 (2001), the dart has a hemispherical nose with a radius of 10.0±0.1 mm. The specimen is clamped between two rectangular steel plates with 13mm thickness and a

central circular cutout of 50.0±0.1 mm. The dart has a weight of 246 g and six additional steel circular plates with a diameter of 75.0±0.1mm and a thickness of 15.0±0.1 mm. They are placed into the rod linked to the dart, as shown in Figure 1. The average weight of each circular plate is 528 g. As the drop weight tower has a maximum height of 3.0 m, the limiting velocity for the device is 7.67 m/s. The dart is made of AISI 4330 steel. The six steel disks can be assembled individually into the dart leading to a mass variation ranging from 246 to 3414 g. During the impact event, the load–time history is recorded by a data acquisition system with a frequency of 50 kHz rate by an A/D data acquisition board. As stated by Found et al. (1998), any digital filtering must be done at a cut-off frequency or below this value, which is in general half of the maximum data acquisition rate. However, as described by Ávila et al. (2007), the cut-off frequency should be l0–15% of the bandwidth of the data in order to avoid problems. In the present case, after a series of pre-tests, a low-pass digital filtering was selected at 3.5 kHz, i.e. 14% of the maximum bandwidth. In contrast with traditional low-velocity impact (LVI) tests performed, the dart is not embraced after the first impact. On the contrary, it is kept free so that it can strike back on the plate as many times as the plate reverses its direction of motion. By applying this tactic, it is possible to evaluate the amount of damage sustained by the sandwich panels.

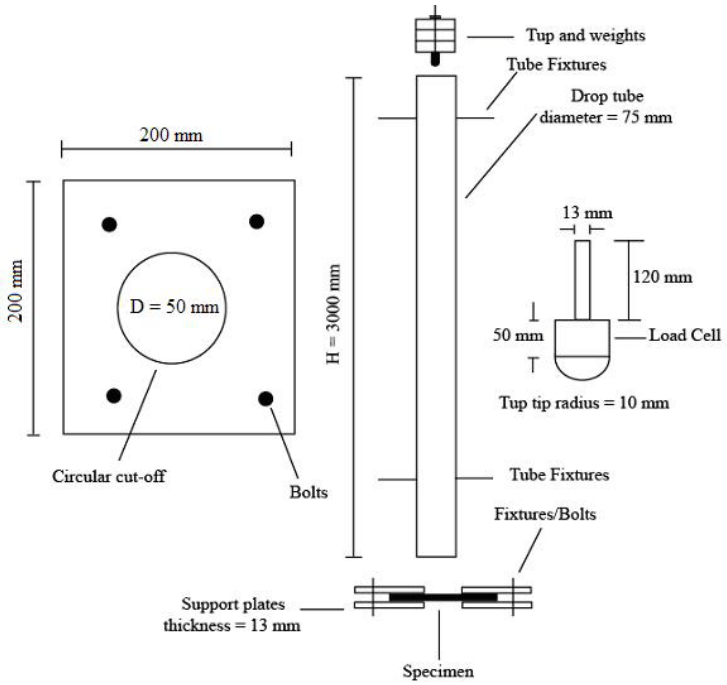

Figure 1. Low velocity impact test scheme.

Following Schubel et al. (2005), the load pulse can be expressed by a half-sine wave as,

$$f(t) = P_0 \sin\left(\frac{2\pi}{T}t\right) \tag{2}$$

By integrating *f(t)* from 0 to T/4, it is possible to obtain the maximum load. The maximum load expression is represented by

$$P_0 = \frac{2\pi mv}{T} \tag{3}$$

Notice that *v* can be obtained by direct measuring or by applying the energy balance equation. Schubel et al. (2005) expressed the incoming velocity in terms of impact energy (*E*) to obtain the maximum load. They described the maximum load as

$$P_0 = \frac{2\pi}{T}\sqrt{2mE} \tag{4}$$

To be able to compute the panel stiffness (k), let's assume that force-deflection response is linear under low velocity impact. From the previous assumption and the pulse duration estimation described by Schubel et al. (2005), the panel stiffness can be calculated by the following equation,

$$k = \frac{4\pi^2 m}{T^2} \tag{5}$$

Perceive that panel stiffness (k) can also be calculated by the slope of static-deflection curve of the upper face sheet. In this research, T is measured directly from the low velocity impact tests and the mass is known. Notice that by substituting equation (5) into the mass spring model described in Mines et al. (1998), equation (3) can be obtained. After the LVI tests the damage was measured using image correlation technique. Public domain image correlation software called ImageJ was employed. At least 10 measurements of each damage area were made and the average and standard deviation were calculated.

4. DATA ANALYSIS

By analyzing Figure 2A, it is possible to conclude that X-ray diffraction (XRD) tests revealed that rather than exfoliated into the epoxy system, the Cloisite 30B nanoclays were in the intercalated form. Another important issue that must be addressed is the matrix saturation limit regarding the nanoclay content. The basal spacing calculated using Bragg's law indicates an increase from 1.35 nm to 1.38 nm when the nanoclay content changed from 5 wt% to 10 wt%. Yet, the amount of nanoclay is twice as much for the 10 wt% nanoclay content specimens and the XRD intensity increases only 57%.

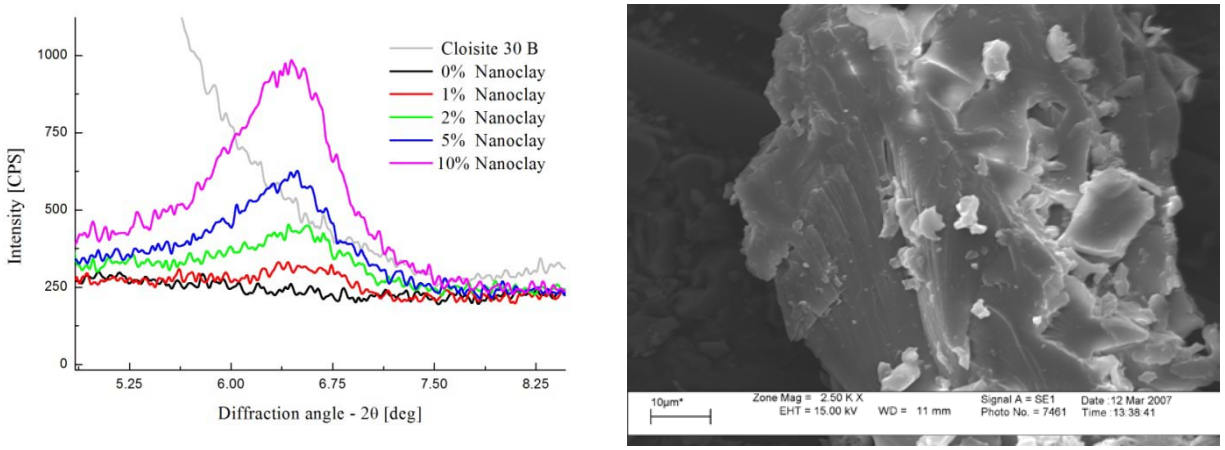

(a) (b)

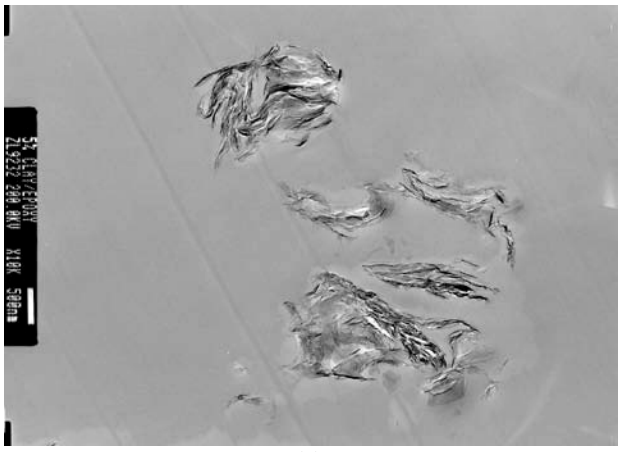

(c)

Figure 2. (a) XRD signature; (b) SEM micrograph showing clusters formation; (c) TEM micrograph with intercalated nano-structures

The unexpected reduction on the diffraction intensity is an indication of a disordered swollen structure, as demonstrated by Fan et al. (2003). Likewise, Ranade et al. (2002) stated that it could be an evidence of a small amount of nanoclay that does not get exfoliated or intercalated, but remains in its own identity leading to an immiscible nano system. This seems the case for the 10 wt% concentration samples. This hypothesis can be visualized in Figures 2B and 2C where the presence of these immiscible nano systems clusters (white regions) and an intercalated nanostructure can be observed. As stated by Luo and Daniel (2006) a partially exfoliated/intercalated system is most likely to occur due to the dispersion system used. In summary, they believed that dispersion process is controlled not only by the nanoparticle morphology but it is also affected by the manufacturing process.

The load-indentation depth curve for the face sheets were obtained based on the methodology described in Zenkert et al. (2004) and the experimental load-central displacement curve. Following the same procedure applied by Tan and Sun (1985), a nonlinear curve fitting is used to obtain the 1.5 power law equations. The results are shown in Figure 3, while the curve fitting parameters are listed in Table 1.

Table 1: Face sheets indentation curve fitting

30B wt%	C [N/mm^n]	n	Ra^2	Average residual
0	286.6419	1.3397	0.9999	1.1085E-7
1	488.5669	1.2509	0.9998	1..7502E-7
2	573.2445	1.1771	0.9992	1.7766E-7
5	521.4524	1.1744	0.9991	1.8446E-7
10	413.9050	1.2690	0.9998	1.7937E-7

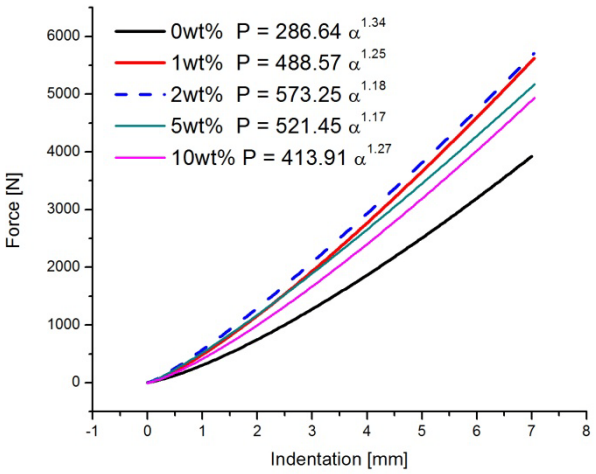

Figure 3. Sandwich panel indentation curves

By analyzing the adjusted coefficient of multiple determinations (Ra^2) and the average residual, it is possible to conclude that not only a good curve fitting was obtained, but it also recognized that the data are not serially correlated. Furthermore, the C coefficients obtained are proportional to the square root of indenter tip, as predicted by Sutherland and Soares (2006) and Shivakumar et al. (1985). Note that for sandwich composites, the n coefficient is lower than 1.5. Hazizan and Cantwell (2002) attributed this lower value to the compliance of the test machine. A more reasonable explanation for the phenomenon was provided by Fatt and Park (2001). According to them, the sandwich panel response can be characterized by the superposition of two effects, that is, the bending of the upper face sheet and the core crushing in the areas below and around the indenter. The core crushing effect is the probable cause of this low value for the n coefficient.

To be able to understand the impact response of sandwich composites with nano-modified face sheets a series of LVI tests were performed. The energies employed were enough to cause damage ranging from a barely visible delamination and perforation. In all cases, the core material is the same; by applying this strategy the core density effect is avoided. Table 2 and 3 show the LVI test parameters. Note that for each energy span, there are two types of impact tests. The first one corresponds to a configuration with the minimum mass (tup + load cell + support) and maximum velocity (condition 1), while the second one is the opposite, i.e. maximum load and minimum velocity. The objective is to investigate the impact velocity and mass effects on damage formation and the sandwich panel response to these variations.

Table 2: LVI test parameters (condition 1)

Energy [J]	Height [m]	Mass [kg]	Velocity [m/s]
25	2.36	1.079	6.80
30	1.91	1.603	6.12
35	2.23	1.603	6.62
40	2.54	1.603	7.06
45	2.15	2.127	6.49
50	2.39	2.127	6.86
55	2.63	2.127	7.18
60	2.30	2.659	6.72
65	2.49	2.659	6.99
70	2.69	2.659	7.26

Table 3: LVI test parameters (condition 2)

Energy [J]	Height [m]	Mass [kg]	Velocity [m/s]
25	0.69	3.717	3.56
30	0.82	3.717	4.02
35	0.96	3.717	4.34
40	1.09	3.717	4.64
45	1.23	3.717	4.92
50	1.37	3.717	5.19
55	1.51	3.717	5.44
60	1.65	3.717	5.68
65	1.78	3.717	5.91
70	1.92	3.717	6.14
75	2.06	3.717	6.35

Figure 4A gives the force versus time data for a 5 wt% panel showing the effects of impact velocity. For lower velocities, i.e. up to 4.34 m/s, the impact period seems to be approximately the same. However, for higher velocities (≥ 5.19 m/s) a decrease on impact period was observed. As it can be noticed in equation (5), stiffness is inversely proportional to the impact period. However, taking into consideration the same panel stiffness, remember we are dealing with panels with 5wt% nanoclay, the decrease on impact period must be explained by the failure mechanism. Higher velocities imply naturally higher energy and a much higher impulse (force/unit of time). A higher impulse will cause a greater localized failure, mainly into core. Core crushing will occur most likely below the tup. This localized core crush contributes to the face sheet failure due to absence of an elastic base.

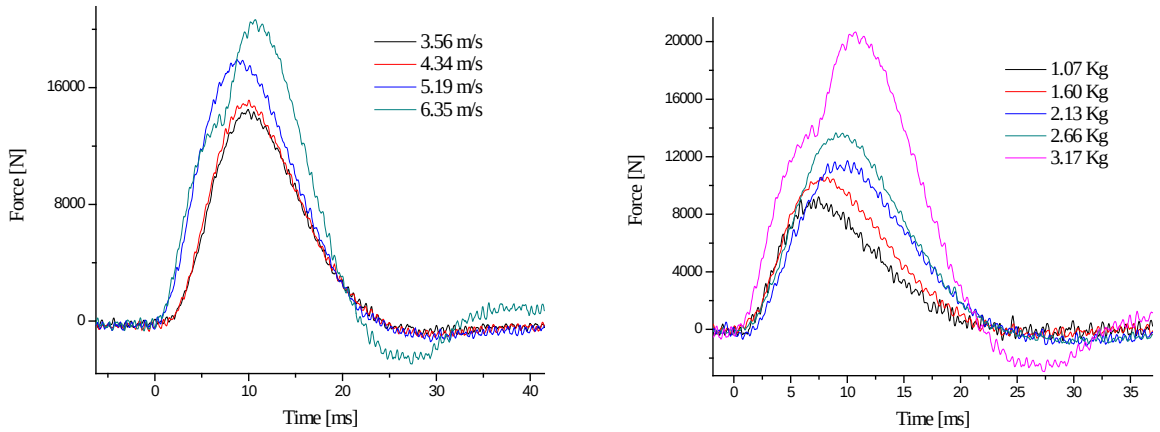

(a) (b)

Figure 4. Force versus time for a 5 wt% panel. (a) Impact velocity effect. (b) Impact mass effect.

Velocities up to 4.64 m/s produced sub-critical damage, i.e. before upper face sheet tearing. At low velocities and consequently small energy levels, a large part of the impact energy is easily dissipated by the face sheet first and the remaining energy is absorbed by core. When the velocity increases to around 5.19 m/s the upper skin tearing and core crushing is observed. This failure mechanism can be explained by a large impulse which caused a high localized

damage, as there was not enough time to impact wave propagation through regions outside below the tup area. This phenomenon is more evident for high energy levels, i.e. >50 J, where the impact wave propagates through the panel thickness right below the tup impact and no significant damage was notice outside the impact projected area. Upper skin tearing and lower skin damage was notice when the velocity reached 5.44 m/s or higher. It is a well known fact that as the energy gets bigger, the damage severity also increases. Perforation with lower skin tearing was experimented for velocities higher than 6.99 m/s. Figure 4B allows us to investigate the mass effect on sandwich panel response to low velocity impact. The velocity was kept higher than 6.3 m/s while the mass changed from 1.08 Kg to 3.7 Kg. The damage caused by these impacts ranged from a barely visible (lower mass) to perforation. As the velocity was kept near constant, the pulse duration could be considered about the same. Another key issue is that face sheet damage mechanism changes with the amount of nanoparticle dispersed.

Figure 5A-C provides the force versus time data for condition 2 where the energies were 25, 50 and 75 joules, respectively. A change on impact pulse is noticed for the 25 joule energy level. According to equation (5), impact pulse is inversely proportional to panel stiffness. Thus, as the panel with 5 wt% nanoclay content has the smallest period (26.89 ms), it must have the largest stiffness. Another interesting issue is that pulse period decreases with the addition of nanoclay up to 5 wt%. The 10 wt% panel has a pulse period 14.96% higher than the 5 wt% panel. The same pattern was noticed for the mid and high range energy, i.e. 50J and 75 J, respectively. As described by equation (5), higher impact period implies into smaller panel stiffness. Therefore, it is possible to conclude that the "extra amount" of nanoparticle did not increase the panel stiffness, in the contrary; it causes a decrease on stiffness. One possible explanation for this phenomenon is the existence of a "saturation" limit of the epoxy system. Once the saturation limit is reached, the additional nanoclay dispersed into the matrix precipitates into the form of immiscible nanostructures, which can be sources of cracks nucleation, as they are stress concentration "hot spots". This hypothesis can be corroborated by the XRD tests, where a significant increase on diffracted energy was notice. Notice that a high diffracted energy is also a sign of large entropy. This increase on entropy can be caused by these precipitated third phase. This hypothesis was confirmed by micrographics using SEM and TEM (figure 1B-C).

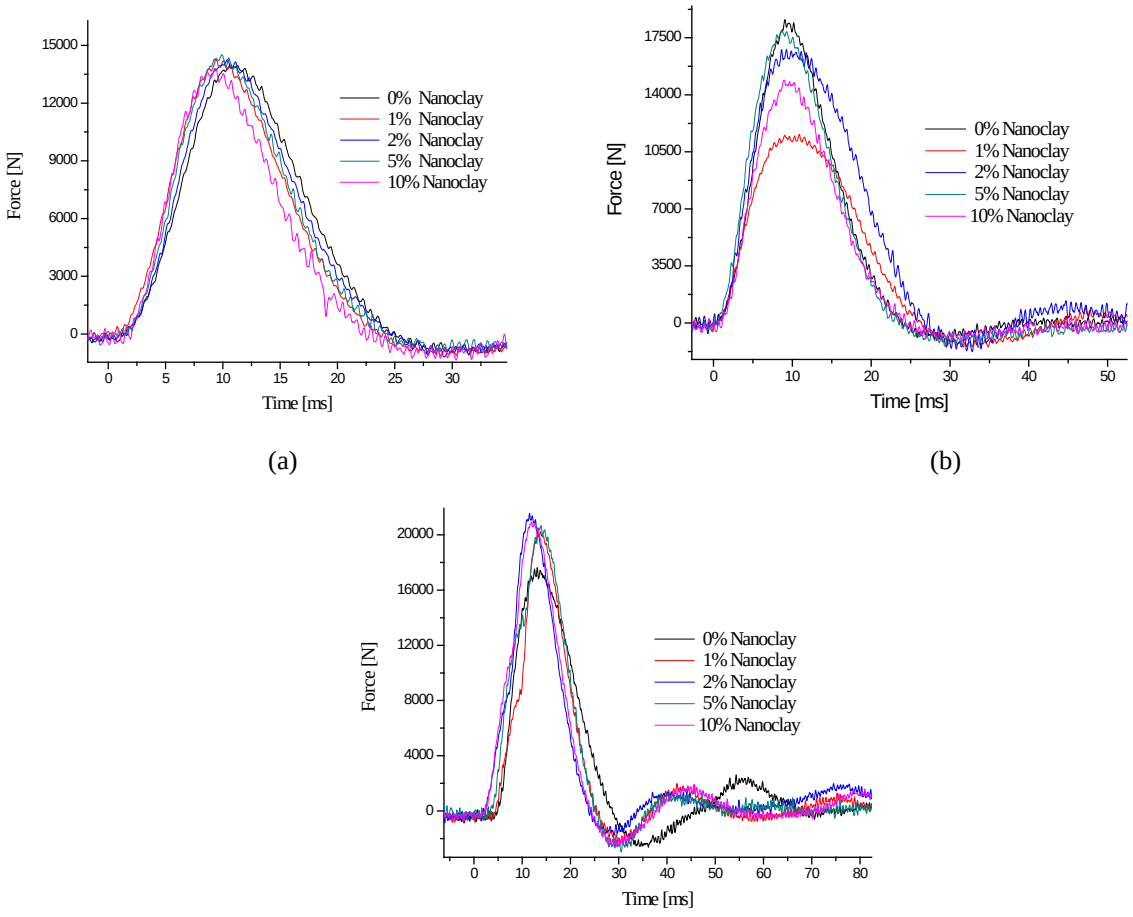

Figure 5. Force versus time data. (a) Low range energy; (b) mid range energy; (c) high range energy

Another important issue is the nanoclay influence into thermal stability. The thermal stability will affect the cure process, which can have direct effect into same laminates properties, such as void formation. According to Avila and

Morais (2009), the void formation is reduced when the nanoparticle dispersed into the laminate increases. As void formation is directed related to the laminate strength, the sandwich panel failure is also related to these issues. A detailed investigation on nanoclay-epoxy composites was performed by Haque and Shamsuzzoha (2003), since they evaluated both mechanical and thermal properties. Their main conclusions were that thermo-mechanical properties mostly increase at low clay loadings (~ 1-2% in weight) but decrease at higher clay loadings (≥ 5% in weight). They also observed a degradation of properties at higher clay loadings. This phenomenon can be due to the phase-separated structures and defects in cross-linked structures. Furthermore, these problems can be caused by the heating phase during the manufacturing process. It is important to mention that in all studies mentioned previously but reference three, heating was present during the nanocomposite synthesis procedure. By abolishing the heating procedure, Ávila et al. (2006) were able to obtain better nanoclay (in their case, Nanomer I30E) dispersion without epoxy system degradation. To achieve such goal, they employed a dispersion technique without heating. The dispersant agent employed was acetone, and the acetone + nanoclay mix was added to the epoxy system hardener and not to the epoxy resin. Mixing the acetone + nanoclay agglomerate to the hardener was easier due to its low viscosity.

Figure 6A-C show the DSC/TGA signature for the pure resin (0wt% nanoclay), 5 wt% and 10 wt% nanoclay, respectively. The addition of nanoparticles, i.e. nanoclay, seems to delay the weight loss. Taking the 410 C temperature, it is possible to observe a weight loss reduction from 46.10% for the pure resin to 36.85% for the 5wt% nanoclay addition. However, an increase on weight loss, i.e. 44.10%, was noticed for the 10wt% nanoclay.

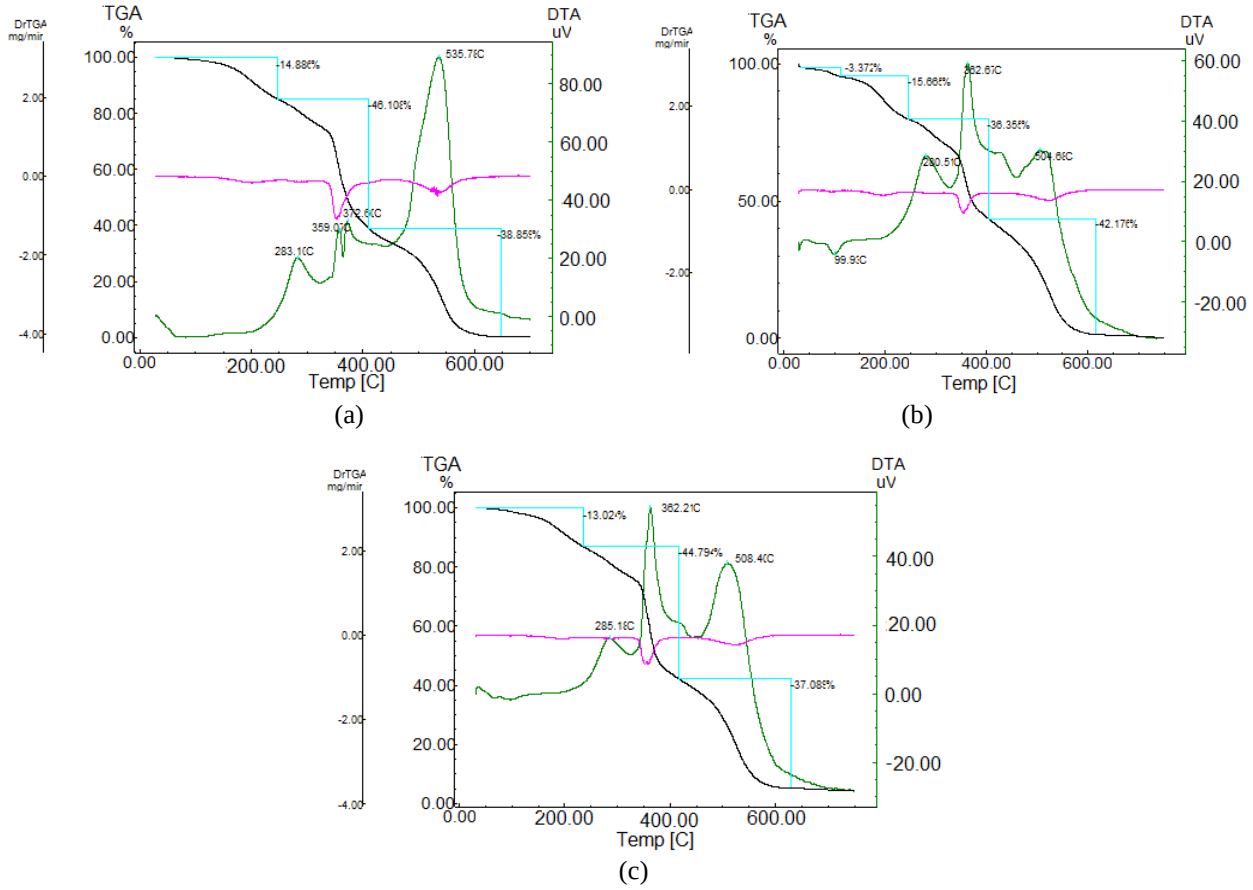

Figure 6. TGA and DTA signatures for nanocomposites with 0 wt%, 5 wt% and 10 wt% nanoclay

However, this increase on weight loss at 410 C is still less the one measured for the pure resin. Based on these results, it is possible to conclude that an improvement in thermal stability similar to that reported by Gilman (1999) is noticed. This increase on thermal stability can be explained by the nanostructures formed inside the epoxy system. Again, the decrease on weight loss for the 10wt% nanoclay content can also be due to the formation of immiscible nanostructures caused by the epoxy system lost of capacity of absorbing more nanoclay. Still, a decrease into glass transition temperature (t_g) was noticed when the nanoparticles are added, i.e. 380 C for the pure epoxy and 360 C for the 1wt% and 2wt% nanoclay content. The glass transition temperature experienced a light increase to 365 C for higher contents of nanoclay. These variations into glass transition temperature (t_g) can be explained by the nanoclay large superficial area which can acts as nucleation sites for polymeric chains. As explained by Ávila et al. (2008), the epoxy system has a saturation limit, it is possible to observe the formation of clusters of immiscible structures.

Damage observed on sandwich panels caused by the tup impact can be classified in six categories: (*i*) barely visible damage; (*ii*) sub-critical damage, i.e. upper face sheet cracking and core indentation; (*iii*) upper face sheet tearing and

core crushing; (*iv*) lower face sheet and core debonding; (*v*) lower face sheet cracking; (*vi*) lower face sheet tearing and perforation. Figure 7A-F shows each one of these categories.

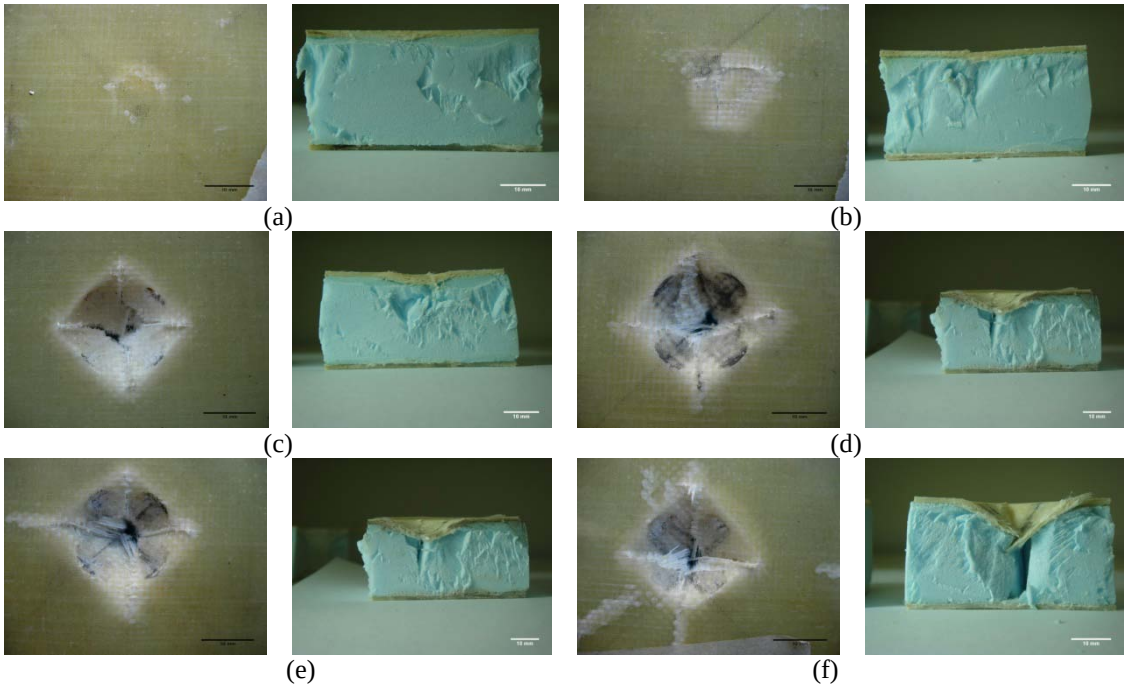

Figure 7. Sandwich panel damage categories

The model predictions (figure 8) were compared against the experimental data with good agreement. However, for large energies (> 50 J), a small deviation was observed. This can be due to the intense core crushing under the impact area. Notice that for the largest energy 75J, a 6% difference between the predicted value and the experimental data is notice. The core crushing rate effect must be included in the present model.

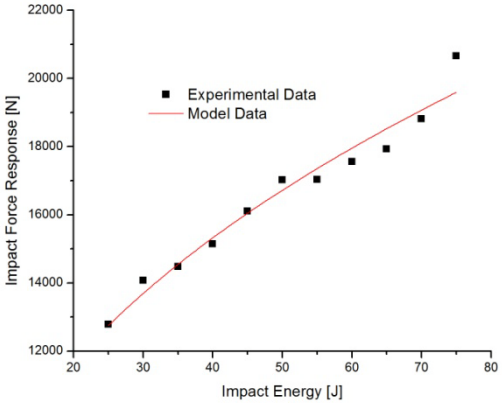

Figure 8. Model prediction versus experimental data

4. CLOSING COMMENTS

The effect of nanoclay addition to fiber glass/epoxy systems and its use on face sheet for sandwich composites was investigated. X-ray diffraction tests and electronic microscopy observation proven the existence of intercalated nano-structures dispersed into the epoxy system. The sudden drop on X-ray diffraction intensity seems to be an evidence of entropy increase as result of an immiscible phase precipitation. It seems that epoxy system has a “saturation” limit between 5 wt% and 10 wt% of nanoclay content. A model to predict the peak reaction for during the low velocity impact was proposed based on pulse duration. The model predictions are limited as the core yielding was not taken into consideration. The addition of nanoclay gives the impression of having effect on pulse duration, as they increase the face sheet laminate stiffness and consequently the panel overall bending rigidity. The pulse period appears to be independent of velocity. Nonetheless, mass changes can affect the pulse period. The nanoclay dispersion on epoxy

system could be the reason for an increase on face sheet stiffness and the panel overall rigidity when low velocity impact tests were performed.

5. ACKNOWLEDGEMENTS

We also would like to acknowledge the financial support provided by the Brazilian Research Council (CNPq) under grants 470511/2006-0, 472213/2007-5 and 300434/2008-1, and the CAPES Foundation.

6. REFERENCES

Abrate, S. 2001. "Modeling of Impacts on Composite Structures," Composite Structures, Vol. 51, n.3, pp.129-138.

ASTM D 5628-01. 2001. "Standard test method for impact resistance of flat, rigid plastic specimens by means of a falling dart (tup or falling mass)," in Annual Book of ASTM Standards.Vol.08 pp.628–637

Ávila, A.F. 2007. "Failure Mode Investigation of Sandwich Beams with Functionally Graded Core," Composite Structures, Vol. 81, n. 3, pp.323-330.

Ávila, A.F. Donadon, L.V. Duarte, H.V. 2008. "Modal Analysis of Nanocomposites Plates," Composite Structures, Vol. 8, n. 3, pp.324-330.

Ávila, A. F. Duarte, H.V. Soares, M.I. 2006. "The Nanoclay Influence on Impact Response of Laminated Plates", Latin American Journal of Solids and Structures, Vol. 3, n. 1, pp.3-20.

Ávila, A. F. Morais, D.T.S. 2009. "Modeling Nanoclay Effects into Laminates Failure Strength and Porosity". Composites Structures, Vol. 87, n. 1, pp. 55-62.

Ávila, A.F. Soares, M.I. Neto, A. S. 2007. "A Study on Nanostructured Laminated Plates Behavior under Low Velocity Impact Loadings," International Journal of Impact Engineering, Vol. 34, n. 1, pp.28-41.

Fan, X. Xia, C. Advincula, R.C. 2003. "Intercalation of Polymerization Initiators into Montmorillonite Nanoparticle Platelets: Free Radical vs. Anionic Initiator Clays," Colloids and Surfaces A, Vol. 219, n.1, pp.75-86.

Found, M.S. Howard, I.C. Paran, A.P. 1998. "Interpretation of Signals from Dropweight Impact Tests," Composite Structures, Vol. 42, n.3, pp.353–363.

Haque, A., and Shamsuzzoha, M., 2003, "S2-Glass/Epoxy Polymer Nanocomposites: Manufacturing, Structures, Thermal and Mechanical Properties," Journal of Composite Materials, Vol. 37, n.. 20, pp. 1821-1837

Hazizan, Md. A. Cantwell, W.J. 2002. "The Low Velocity Impact Response of Foam-Based Sandwich Structures," Composites Part B, Vol. 33, n.2, pp.193-204.

Laurin, F. Vizzini, A.J. 2005. "Energy Absorption of Sandwich Panels with Composite-Reinforced Foam Core," Journal of Sandwich Structures and Materials, Vol. 7, n.1, pp.113-131.

Li, Q.M. Ma, G.W. Ye, Z.Q. 2006. "An Elastic-Plastic Model on the Dynamic Response of Composite Sandwich Beams Subjected to Mass Impact," Composite Structures, Vol. 72, n.1, pp.1-9.

Lim TS, Lee CP, Lee DG. 2004. "Failure Modes of Foam Core Sandwich Beams under Static and Impact Loads," Journal of Composite Materials, Vol. 38, n. 18, pp.1639–1662.

Luo, J-J. Daniel, I.M. 2003. "Characterization and Modeling of Mechanical Behavior of Polymer/Clay Nanocomposites," Composites Science and Technology Vol. 63, n.10, pp.1607-1616.

Koo, J.H. 2006. Polymer Nanocomposites : Processing, Characterization, and Applications. McGraw-Hill New York.

Mines, R.A.W. Worrall, C.M. Gibson, A.G. 1998. "Low Velocity Perforation Behavior of Polymer Composite Sandwich Panels," International Journal of Impact Engineering, Vol. 21, n.10, pp.855-879.

Ranade, A. D'Souza, N.A. Gnade, B. 2002. "Exfoliated and Intercalated Polyamide-Imide Nanocomposites with Montmorillonite," Polymer Vol. 43, n. 10, pp.3759-3766.

Schubel, P.M. Luo, J.-J. Daniel, I.M. 2005. "Low Velocity Impact Behavior of Composite Sandwich Panels," Composites Part A, Vol. 36, n.11, pp.1389-1396.

Shivakumar, K.N. Elber, W. Illg, W. 1985. "Prediction of Impact Force and Duration Due to Low-velocity Impact on Circular Composite Laminates," Transactions ASME Journal of Applied Mechanics, Vol. 52,n.2, pp.674-680.

Suvorov, A.P. Dvorak, G.J. 2005. "Enhancement of Low Velocity Impact Damage Resistance of Sandwich Plates," International Journal of Solids and Structures, Vol. 42, n.16, pp.2323-2344.

Tan, T.M. Sun, C-T. 1985. "Use of Static Indentation Laws in the Impact Analysis of Laminated Composite Plates," Transactions ASME Journal of Applied Mechanics, Vol. 52, n.1, pp.6–12.

Vinson, J. R. 1999. The Behavior of Sandwich Structures of Isotropic and Composite Materials. 2nd ed. Technomic.

Zenkert, D. Shipsha, A. Persson K. 2004. "Static Indentation and Unloading Response of Sandwich Beams," Composites Part B, Vol. 35, n. 5, pp.511-522.

7. RESPONSIBILITY NOTICE

The authors are the only responsible for the printed material included in this paper.